Cathode interface engineering for stable and efficient organic light-emitting diodes

Yong Qiu, Lian Duan and Yang Li*
Key Lab of Organic Optoelectronics & Molecular Engineering of Ministry of Education, Department of Chemistry, Tsinghua University, Beijing 100084, China
TEL:86-10-6277-1964, e-mail: qiuy@mail.tsinghua.edu.cn

Keywords : electron injection, organic light-emitting diodes, interface

Abstract

The improvement of the electron injection is of critical importance for obtaining efficient and stable organic light-emitting diodes(OLEDs). Here, we report some of our recent results on the development of new cathode interlayer materials for OLEDs. Some of our new materials show performance superior to that of LiF.

1. Introduction

The improvement of the electron injection system is of critical importance for obtaining highly efficient low-voltage OLEDs [1]. In general, low work function metals such as Ca (2.9eV), Mg (3.7eV), Li (2.9eV), or Cs (2.1eV) are used as the cathode for OLEDs to reduce the electron injection barrier and improve the device efficiency. However, reactive metals with a low work function are difficult to handle because they are always susceptible to atmospheric moisture and oxygen. An alternative approach to improve electron injection is by an interface modification method. It is well known that electron injection into tris-(8-hydroxyquinoline) aluminum (Alq_3) is improved by insertion of a thin lithium fluoride (LiF) interlayer between the Al cathode and Alq_3 layer[2]. However, from the scientific point of view, LiF/Al cathode system is far from ideal in that: 1) the evaporation temperature of LiF is very high; 2) Li atoms can be released from the LiF only in the presence of Al and Alq_3[3], and therefore LiF/Al may not be a "universal solution".

In this work, we report some of our work on the development of new electron injection materials(EIM) based on alkali metal complexes[4] and decomposable alkali compounds[5] for organic light-emitting diodes. They all have lower evaporation temperature than LiF and some of these materials show performance superior to that of LiF.

2. Organic metal complex for EIM

Comparing the inorganic compounds, alkali metal complexes with organic ligands, such as lithium quionlate (Liq)[6], have shown many advantages such as lower deposition temperature and higher electron transporting properties. Here, we report our results on a novel lithium complex containing quinoxaline moiety as the EIM for improved electron injection.

LiDPQX was synthesized by treating 2,3-diphenyl-5-hydroxyquinoxaline and the equal mole amount of $LiOH{\cdot}H_2O$ in a CH_2Cl_2 solution. After 90 hours of stirring at room temperature, the precipitated yellow powder was filtered, and further purified by the train sublimation.

Figure 1 shows the chemical structure and the optimized geometry of the LiDPQX molecule. The geometry optimization and the property calculation of LiDPQX were performed by using the GAUSSIAN 03 package at B3LYP/6-31g(d) level. It can be seen from the geometry configuration that the presence of the two nonplanar phenyl moieties can reduce the intermolecular interaction of the quinoxaline moieties due to the steric hindrance, and enable easy evaporation of LiDPQX in vacuum.

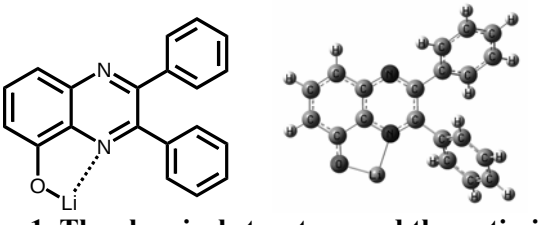

Fig. 1. The chemical structure and the optimized ge ometry of the LiDPQX molecule.

A set of NPB 50nm/Alq_3 nm devices with various thicknesses (0 nm, 0.5 nm, 1.0 nm, 2.0 nm, and 3.0 nm) of LiDPQX as EIM were prepared and tested. The electroluminescent (EL) efficiency of OLEDs became higher when the thickness of LiDPQX

increased to the optimum one of 1.0 nm, and further increase in thickness resulted in the decrease of the device performance. For comparison, two control devices with LiF 0.5 nm/Al (Device B) and with only Al as cathode (Device C) were also fabricated. The L~V and J~V characteristics of the device with 1.0 nm of LiDPQX as EIM (Device A) and the two control devices (Devices B and C) are illustrated in Figure 2. It can be seen that the L~V and J~V curves of Device A both shift to lower voltage range compared with the Devices B and C. In Device A, a high luminance of 26,000 cd/m^2 is observed at 12 V. The turn-on voltage (the voltage required for 1 cd/m^2) drops from 3.9 V to 3.4 V when the LiDPQX was inserted to replace LiF. The maximum power efficiencies of Devices A, B, and C are 1.19 lm/W, 0.93 lm/W, and 0.35 lm/W, respectively. Again, Device A shows the best performance.

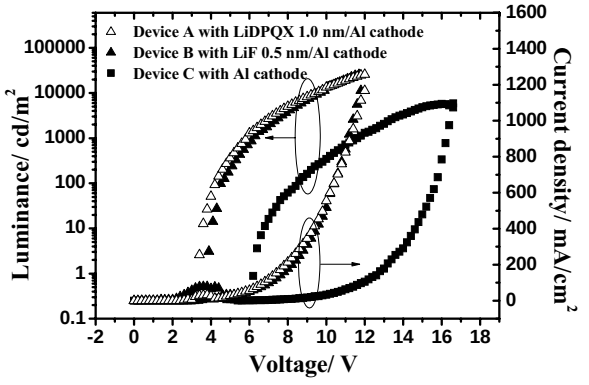

Fig. 2. Plots of luminance vs. voltage (L~V) and current density vs. voltage (J~V) characteristics obtained from OLEDs A, B and C

As an electron injection material the LiDPQX has two advantages over LiF: First, LiDPQX is a kind of semiconductor which has a proper LUMO energy level to facilitate the electron injection. The HOMO energy level of LiDPQX, measured with the typical cyclic voltammetry (CV) and calculated with reference to ferrocene (Fc), was determined to be -4.90 eV. The optical edge of LiDPQX film in the UV-vis spectrum was utilized to derive the bandgap (2.40 eV). This value, together with the HOMO energy level, was used to calculate the LUMO energy (-2.50 eV), which is very close to the LUMO energy of Alq_3 (-2.55 eV). It suggests that electrons can easily be injected from LiDPQX to Alq_3 layer, even at low current density driving condition, due to the extremely low energy barrier. When LiF is used as EIM, however, due to its insulating property with a high band gap of 12 eV, even 0.5-nm-thick LiF will introduce an extra electron injection barrier at the cathode interface, which can reduce the electron injection at low current density driving condition and lead to the lower device efficiency.

Second, in the LiF/Al composite cathode the chemical reaction between LiF and Al is thermodynamically inhibited. This reaction doesn't occur until it is cooperated with the formation of Alq_3 anion from Alq_3 due to extra energy released during the electron acception process, as shown in Equation (1).

$$Al + 3LiF + 3Alq_3 \rightarrow AlF_3 + 3Li^+Alq_3^-. \quad (1)$$

In the LiDPQX/Al composite cathode, it is predicted that the extra energy can also be released when LiDPQX accepts an electron. This prediction can be testified by the quantum computation. For the Alq_3 and LiDPQX molecules, it can be calculated that their anions are energetically more stable than the neutral species, and they have almost the same energy released when the neutral molecules change to anions. Here an unrestricted DFT (UB3LYP/6-31g(d)) method was used to obtain the absolute energies of the neutral molecule and anion of LiDPQX. The total energy difference between the LiDPQX anion and its neutral molecule was calculated to be 0.60 eV. In the case of Alq_3, this energy difference was determined to be 0.55 eV by Qiao *et al.*[7] using the same computation method. It therefore suggests that the liberation of Li atoms and the formation of LiDPQX anions are able to take place even in the absence of Alq_3 at the cathode interface unlike the case when LiF is used as EIM, as shown in Equation (2).

$$Al + 6LiDPQX \rightarrow Al(DPQX)_3 + 3Li^+(LiDPQX)^-. \quad (2)$$

Further investigation is underway to test this possibility.

3. Alkali Metal Precursors for EIM

There have been several attempts to use alkali compounds that will decompose to form alkali metal during vacuum thermal evaporation[8]. In this approach, the decomposable alkali compounds should be carefully chosen, otherwise the harmful gases produced during decomposition and/or the possible residues left in the crucible might be a big problem for the OLED fabrication. Moreover, it is difficult to

measure the decomposition processes in situ and therefore difficult to understand the mechanisms. In this work, we report the use of an improved QCM method to investigate the possible evaporation behavior of the alkali compounds. Relationship between the shift of the frequency of the quartz crystal and the mass loss in the crucible can be used to measure whether decomposition happened during evapration. In order to reduce the experimental errors, we compared the slope of the linear relationship (frequency shift vs. mass loss) of alkali compounds with the slopes of those of thermally stable materials of LiF and CsF.

Δf can be converted to the mass load on the surface of the quartz crystal wafer using the standard Sauerbrey formula[9] as follows:

$$\Delta f = -2.26\times10^{-6} f^2 \Delta m / A, \quad (3)$$

where Δf (Hz) denotes the change in the oscillation frequency of the quartz crystal; f (Hz), the resonance frequency of the quartz crystal; Δm (g), the change in the mass adsorbed onto the crystal; and A (cm^2), the deposition area on the quartz crystal.

During evaporation, if the source material is thermally stable, the mass adsorbed onto the crystal surface (Δm) would be in direct ratio to the mass loss in the crucible (ΔM):

$$\Delta m = -k\Delta M \ (k \geq 0). \quad (4)$$

Then, we get Equation (5):

$$\Delta f = K\Delta M \quad K = 2.26\times10^{-6} f^2 k / A. \quad (5)$$

Here, K is a positive constant that is independent of the materials used. It can be seen that Δf is in direct ratio to ΔM. On the contrary, if the source material decomposes and only a fraction (d%) is deposited, Δf would be in direct ratio to d% × ΔM:

$$\Delta f = d\%K\Delta M \quad K = 2.26\times10^{-6} f^2 k / A. \quad (6)$$

It is clear that the slope of the line (Δf~ΔM) may decrease to d% of its initial value if the source material decomposes.

We introduced approximately 10 mg, 20 mg, 30 mg, and 40 mg of LiF (Aldrich, random crystals), CsF(Aldrich, >99.99%), Li_3N(Aldrich, >99.9%) and Cs_2CO_3(Alfa Aesar, > 99.9%), respectively, into the BN crucible in the vacuum chamber. The resistive heating was controlled by adjusting the source current (I) of the power supply (0–170 A). The QCM device used was a conventional thickness monitor operating at a resolution and frequency stability of ±1Hz. The QCM was placed at approximately 300 mm above the crucible and was water cooled to reduce the surface temperature.

The Δf vs. ΔM characteristics are shown in Fig. 3. There is little mass change of the crucible after completion of evaporation.

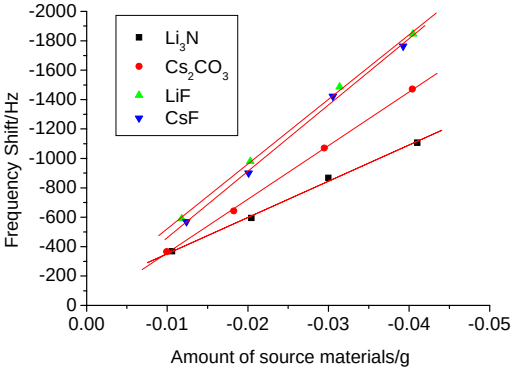

Fig. 3 The frequency shift (Δf) vs. mass loss (ΔM) characteristics

The slope of LiF and CsF are almost identical, indicating that the non-decomposable behaviors of LiF and CsF. In the cases of Li_3N and Cs_2CO_3, we can see that the negative Δf values are less than those of LiF and CsF. And we get the fractions (d%) deposited on to the quartz crystal to be 56.1% and 80.9% for Li_3N and Cs_2CO_3, respectively.

If the following reaction happens:

$$2Li_3N \rightarrow 6Li + N_2\uparrow \quad (6)$$

then d% can be calculated to be 59.8 %. It is clear that the experimental result well agrees with the calculated one, indicating that metallic lithium is deposited on the substrate during the thermal evaporation of Li_3N in vacuum.

And for Cs_2CO_3:

$$2Cs_2CO_3 \rightarrow 4Cs + O_2\uparrow + 2CO_2\uparrow. \quad (7)$$

From the above equation, we get a d% value is 81.6%, which agrees well with the experimental result. Thus, we conclude that the highly reactive cesium metal is deposited on the Alq_3 layer and provides electrons to the Alq_3 matrix to form a highly efficient electron injection contact.

As Li_3N and Cs_2CO_3 decompose to form alkali metal, the efficient electron injection contact should generate as soon as Li_3N or Cs_2CO_3 is evaporated. Therefore, the device performance should be independent to the work function of the additional metal layer. We fabricated a series of OLEDs (NPB 50 nm/Alq_3 50 nm) with the following cathode structures:
Device D: Li_3N 1 nm/Al 120 nm,
Device E: Li_3N 1 nm/Ag 120 nm,
Device F: Cs_2CO_3 1 nm/Al 120 nm,
Device G: Cs_2CO_3 1 nm/Ag 120 nm.
The L~V and J~V characteristics of Devices D~G are plotted in Fig. 4. The active area of the device was set to be 3 × 3 mm^2 by a metal mask. The current density vs. voltage and luminance vs. voltage (J~V and L~V) characteristics of the devices were measured at room temperature under ambient conditions with a Keithley model 4200 source-measure unit and a calibrated silicon photodiode. As can been seen from Fig. 4, the performances of all the devices are almost the same, confirming the decomposition mechanism of the alkali precursors during evaporation.

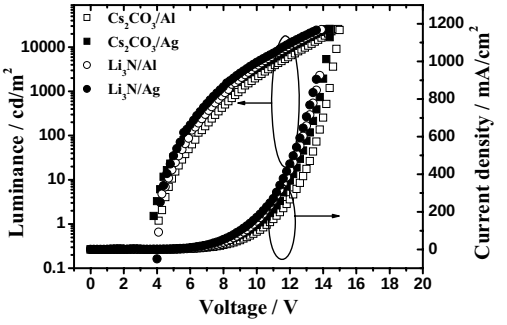

Fig. 4 The luminance vs. voltage and current density vs. voltage characteristics of the OLEDs.

4. Summary

We have fabricated efficient OLEDs using both alkali metal complex (LiDPQX) and decomposable alkali precursors (Li_3N and Cs_2CO_3) as the electron injection material instead of LiF. Our results demonstrated that they are all promising EIM for OLEDs.

5. References

[1] C. W. Tang and S. A. Vanslyke, Appl. Phys. Lett. **51**, 913 (1987)

[2] L. S. Hung, C. W. Tang, and M. G. Mason, Appl. Phys. Lett. 70, 152 (1997)

[3] L. S. Hung, R. Q. Zhang, P. He, and G. Mason, J. Phys. D: Appl. Phys. 35, 103 (2002)

[4] L. Li, D. Q. Zhang, L. Duan, R. Zhang, L. D. Wang, J. Qiao, and Y. Qiu, Japn. J. Of Appl. Phys. Part 2, 45, L1253 (2006)

[5] L. Li, D. Q. Zhang, L. Duan, R. Zhang, L. D. Wang, and Y. Qiu, Appl. Phys. Lett. 90, 012119 (2007)

[6] J. Endo, J. Kido and T. Matsumoto, Ext. Abstr. (59th Autumn Meet.); Japan Society of Applied Physics, 1086(1998)

[7] J. Qiao, H. Tan, Y. Qiu and K. J. Balasubramanian: J. Chem. Phys. **124** 024719(2006)

[8] C. Ganzorig and M. Fujihira, Appl. Phys. Lett. 85, 4774 (2004)

[9] T. Hasegawa, S. Miura, T. Moriyama, T. Kimura, I. Takaya, Y. Osato, and H. Mizutani, SID Int. Symp. Digest Tech. Papers 35, 154 (2004)